# β1 integrin inhibition dramatically enhances radiotherapy efficacy in human breast cancer xenografts

Catherine C. Park, Hui J. Zhang, Evelyn S. Yao, Chong J. Park, Mina J. Bissell

Correspondence:

Catherine Park, M.D.

Assistant Professor

UCSF Comprehensive Cancer Center

Department of Radiation Oncology

1600 Divisadero St. H1031

San Francisco, CA 94143-1708

Telephone: 415-353-7175

Fax: 415-353-9883

Email: Catherine.Park@ucsf.edu

**Abstract**

β1 integrin signaling has been shown to mediate cellular resistance to apoptosis after exposure to ionizing radiation (IR). Other signaling molecules that increase resistance include Akt, which promotes cell survival downstream of β1 integrin signaling. We showed previously that β1 integrin inhibitory antibodies, AIIB2, enhance apoptosis and decrease growth in human breast cancer cells in 3 dimensional laminin-rich extracellular matrix (3D lrECM) cultures and *in vivo*. Here we asked whether AIIB2 could synergize with IR to modify Akt-mediated IR resistance. We used 3D lrECM cultures to test the optimal combination of AIIB2 with IR treatment of two breast cancer cell lines, MCF-7 and HMT3522-T4-2, as well as T4-2 myr-Akt breast cancer colonies or HMT3522-S-1, which form normal organotypic structures in 3D lrECM. Colonies were assayed for apoptosis and β1 integrin/Akt signaling pathways were evaluated using western blot. In addition, mice bearing MCF-7 xenografts were used to validate the findings in 3D lrECM. We report that AIIB2 increased apoptosis optimally post-IR by down regulating Akt in breast cancer colonies in 3D lrECM. *In vivo*, addition of AIIB2 after IR significantly enhanced tumor growth inhibition and apoptosis compared to either treatment alone. Remarkably, the degree of tumor growth inhibition using AIIB2 plus 2 Gy radiation was similar to that of 8 Gy alone. We showed previously that AIIB2 had no discernible toxicity in mice; here, its addition allowed for a significant reduction in the IR dose that was necessary to achieve comparable growth inhibition and apoptosis in breast cancer xenografts *in vivo*.

## Introduction

Radiation therapy is an effective modality used for breast cancer treatment, however, tumor resistance and recurrences remain significant clinical problems(1). Increasing evidence indicates that in addition to DNA damage, multiple cellular mechanisms such as cell interactions with neighboring cells and the microenvironment fundamentally influence cell fate in response to ionizing radiation (IR) (2). Indeed, single doses of IR to single cells could modify cell-cell and cell-extracellular matrix (ECM) interactions and confer heritable epigenetic traits (3).

Adhesion to ECM has long been known to modify radiation sensitivity in several cell types, including cancer. Integrins, a major class of transmembrane molecules that mediate adhesion and cell-ECM interactions are aberrantly expressed in many cancer cell types, and are upregulated post-IR(4, 5). In particular, β1 integrins have been found to be upregulated by clinically relevant doses of IR in cancer cell lines (4) and in human mammary epithelial cells in 3 dimensional laminin rich extracellular matrix (3D lrECM) cultures (3, 5). β1 integrins have been implicated in mediating resistance to IR (6-10); However, the role of β1 integrins as a strategic molecular target in conjunction with IR has not been fully investigated.

β1 integrins belong to a family of heterodimeric receptors whose ligands are arginine-glycine-aspartic acid (RGD) -containing ECM molecules(11). Acting largely as mechanoreceptors, β1 integrins transmit biochemical cues that can facilitate multiple cellular fates downstream, including apoptosis and survival(12).

Increase in β1 integrins appear to enhance cancer cell viability by promoting survival, and confer resistance to chemotherapy in several tumor cell types (10, 13, 14). In addition, we have shown previously that in a subset of patients with early stage breast cancer, high β1 integrin expression is associated with poor overall survival, indicating that this subgroup of patients may benefit from more aggressive and targeted therapy (15).

Cancer cell resistance to IR has been shown previously to be mediated via Akt, a serine threonine kinase that lies immediately downstream of phoshatidyl-inositol-3 (PI3) kinase and the integrin signaling pathways (16, 17). β1 integrin has been shown to enhance cancer cell survival via the PI3 kinase pathway in lung cancer(10) and in normal fibroblasts (18) in culture. We have shown previously that β1 integrin inhibitory antibodies selectively induce apoptosis in breast cancer cells but not non-malignant acini in 3D lrECM cultures; these findings were validated *in vivo* with no toxicity to animals (19), indicating that β1 integrin is a highly promising therapeutic target. In this report, we used the 3D lrECM assay and *in vivo* models of breast cancer to test the hypothesis that β1 integrins may facilitate IR-induced resistance by promoting Akt-mediated survival.

## Materials and Methods

### Cell Culture

Non malignant human mammary epithelial cells, HMT-3522 (S-1), were originally derived from a woman with fibrocystic breast disease (20), and were

cultured in H14 medium (21). S-1 cells were propagated on plastic in medium containing 10ng/ml EGF. Also derived from the same parental line, malignant HMT-3522 (T4-2) cells were propagated on collagen type I-coated flasks in the absence of EGF(21). T4-2 wild type cells that were either stably transfected with a constitutively active myristoylated Akt (T4-2 myrAKT) or empty vector control (T4-2 vc) were a gift from Hong Liu, UCSF. Human breast cancer cell line, MCF-7, was obtained from ATCC (Manassas, VA). Three dimensional laminin-rich extracellular matrix (3D lrECM) cultures consisted of cells trypsinized from monolayer cultures and plated on top of commercially available gel produced from Englebreth-Holm-Swarm tumors (Matrigel; BD Sciences, San Jose, CA). Cell lines were maintained in H 14 media as described previously (19) and transferred to the modified 3D lrECM assay (19). This is referred to as Day 0. Cultures were exposed to ionizing radiation (IR) and/or AIIB2 on Day 6 of culture after acinar formation for non-malignant S1 cells and on days 4 and 5 of culture, sequentially for malignant cell lines. AIIB2 was added to culture medium on alternate days. All cultures were analyzed 72 hours after the first treatment.

**AIIB2**

β1 integrin function-blocking antibody, clone AIIB2, was originally a purchased gift from Carolyn Damsky at UCSF. AIIB2 is a rat monoclonal $IgG_1$ that was isolated from a human choriocarcinoma hybridoma that specifically binds β1 integrin extracellular domain (22-24). Prior experiments using $F(ab')_2$ fragments of enzyme-digested AIIB2 indicated that the epitope-binding portion of

the antibody was active, and resulted in down-modulation of β1 integrin-mediated signaling (21, 25).

**Apoptosis and Proliferation Assays in 3D lrECM**

Proliferating cells from 3D lrECM cultures were detected by indirect immunoflourescence of Ki-67 nuclear antigen. Samples taken from cultures were fixed onto glass slides using methanol/acetone and blocked in 10% goat serum for one hour at room temperature in a humidified chamber. Slides were then incubated in primary rabbit antibody against Ki-67, clone MIB-1, (Novocastra Laboratories, Norwell, MA) for 1 hour. After washing in PBS, FITC-conjugated anti-rabbit secondary antibody (Jackson Laboratories, Bar Harbor, ME) was applied for 1 hour in a dark humidified chamber. Slides were then washed and counterstained with DAPI before mounting with Vectashield mounting medium (Vector Laboratories, Burlingame, CA). Apoptosis was assayed by detecting terminal deoxynucleotidyl transferase-mediated dUTP nick end labeling (TUNEL) in samples taken from 3D lrECM cell culture using a commercially available kit (In Situ Cell Death Detection Kit, Fluorescein; Roche, Nutley, NJ). Samples from cultures were fixed onto glass slides in 4% paraformaldehyde and permeabilized in 0.1% Triton X-100 in 0.1% sodium citrate. After washing, cells were incubated in TUNEL reaction mixture at 37ºC for 60 minutes and mounted.

**Fluorescence Activated Cell Sorting (FACS) Analysis**

S-1 and T4-2 cells grown on tissue culture plastic were harvested using 0.25% trypsin. After resuspending cells in DMEM/F-12 media containing trypsin inhibitor, cells were spun down and washed in 5% fetal bovine serum and 0.1% sodium azide in PBS on ice. Cells were incubated first in dilute primary Annexin V antibody (Trevigen, Gaithersberg, MD) for at 4°C for 30-60 minutes, then washed and incubated with a flourescein-conjugated IgG secondary antibody (1:100) for 30-60 minutes. After washing, the pellet was immediately suspended in 1% paraformaldehyde. Cells were analyzed using a Beckman-Coulter EPICS XL-MCL Analyzer. System II Data Acquisition and Display software, version 2.0 was used for data analysis.

**Colony forming assays**

T4-2 and S-1 cells were propagated on 2D as previously described (21). After reaching 50-70% confluence, culture flasks were exposed to IR (Sham, 2, 4 or 8 Gy). Six hours later, they were trypsinized and replated onto 35mm per well dishes and allowed to grow for 10-12 days. Dishes were treated with crystal violet and colonies with greater than 50 cells were counted. Six wells per condition were plated for n=3 experiments. Plating efficiencies and surviving fractions were estimated based on binomial probability distribution.

**Western Immunoblot**

To release cells from 3D lrECM, cultures were first treated with ice-cold PBS/EDTA (0.01M sodium phosphate [pH 7.2] containing 138 mM sodium

chloride and 5mM EDTA) and then lysed in RIPA buffer as previously described(21). Protein was aliquoted onto reducing SDS gels in equal amounts and separated using low voltage current. Protein bands were transferred onto nitrocellulose membrane (Invitrogen, Carlsbad, CA), and blots were blocked with 5% nonfat milk. Blots were probed with antibodies as listed below, then washed, incubated with secondary antibody and exposed to x-ray film. Antibodies used included β1 integrin, Clone 18 (Oncogene, Cambridge, MA); FAK, Clone 77 (BD Transduction Laboratories, San Diego, CA); phospho-FAK, Clone 14 (BD Transduction Laboratories, San Diego, CA); AKT, Clone 7 (BD Transduction Laboratories, San Diego, CA); phospho-AKT (Cell Signaling, Danvers, MA); phospho-β1 integrin (Biosource Camarillo, CA); TSC-2 clone c-20 (Santa Cruz Biotechnology, Santa Cruz, CA); phospho-Thr 1462-TSC-2: (Catalog # 9315, Cell Signaling, Danvers, MA); β actin: Clone AC-15, (Sigma, Saint Louis, Missouri); secondary ECL anti-rabbit IgG/ ECL, anti-mouse IgG (Amersham, Piscataway, NJ).

**Tumor growth and toxicity assessment *in vivo***

Female Balb/c $nu^{-/-}$ congenic mice were obtained from Simonsen Laboratories (Wilmington, MA) and kept in a controlled animal barrier at five per cage with water and chow as needed. After one week, animals were injected subcutaneously with $10^7$ MCF-7 cells into the posterior rear flank. Estradiol pellets were inserted subcutaneously above the tail for animals bearing MCF-7 xenografts. AIIB2 antibody or non-specific rat IgG was injected into the

intraperitoneal cavity bi-weekly beginning on Day 7-8 after cell implantation, before or after IR exposure. Prior to irradiation, animals were restricted in a Lucite container and the upper hemi-torso was shielded using 1.0 cm thick cerrobend. Ionizing radiation was delivered to the exposed tumor and posterior hemi-torso using a 250 kVP source. Bi-weekly tumor dimensions (width, height and depth) were recorded. At the time of sacrifice, animals were euthanized, and tumors were harvested and either immediately snap frozen or fixed in formalin. Animals were monitored for toxicity by measuring weight, assessing overall activity, and necropsy. All experimental procedures received prior approval by the Lawrence Berkeley National Laboratory Animal Welfare and Safety Committee.

**Detection and Quantification of Ki67 and TUNEL on in vivo tumor sections**

We have developed methods to detect dual immunofluorescence of Ki-67 and TUNEL (adapted from Schafer et. al. (26)) in paraffin-embedded tissues that will allow simultaneous evaluation of the patterns of proliferation and apoptosis in situ. Five micron sections from each tumor were baked in a 60˚C oven for 30 minutes, dewaxed in xylene, and rehydrated through graded alcohols. Antigen retrieval was accomplished by heating slides in 10mM sodium citrate buffer, pH 6.0, for 45 minutes at 95-97°C. After cooling for 30 minutes at room temperature, sections were washed and then blocked in 10% goat serum/PBS for 1 hour. Primary antibody against Ki67 (Vector, Burlingame, CA) is diluted in 10% goat serum/PBS, applied to the slide, and incubated overnight at 4°C. Slides were

washed and incubated with Alexa Fluor 594 conjugated goat anti-rabbit IgG (Molecular Probes, Carlsbad, CA) and diluted in 10% goat serum/PBS for 40 minutes at room temperature. Slides are subsequently washed and labeled with 4',6-diamidino-2-phenylindole (DAPI). Primary antibody was withheld from negative controls.

After verification of staining, coverslips were removed and sections were washed thoroughly with PBS. All samples were permeabilized in freshly prepared 0.1% Triton X-100, 0.1% sodium citrate in $H_2O$ for 10 minutes at room temperature. Slides were then blocked for 1hour in 3% BSA, 20% FBS, 0.1M Tris-HCL, pH 7.5 and washed with PBS. To detect apoptosis, we used In Situ Cell Death Detection Kit, Fluorescein (Roche, Nutley, NJ). A TUNEL reaction mixture of label and enzyme solution was incubated on each slide for 1hour in a dark, 37°C incubator. Negative controls were incubated with label solution only. After washing in PBS, slides were labeled again with DAPI, mounted with Vectashield. Lymph node tissue was used as a positive control for both Ki67 and TUNEL staining.

After staining, fluorescent images were acquired on a Zeiss Axioplan 2 Imaging microscope and AxioCam camera. Five representative images will be obtained for each tumor using a 40x oil objective and 10x eyepiece for a total magnification of 400x. All final images consist of a composite of three different exposures: DAPI (nuclei), FITC (TUNEL), and Cy3 (Ki67).

MetaMorph® software was employed to quantify the number of positive versus total nuclei present in each image composite. For each image, a DAPI

“mask” was created by accounting for all the nuclei from the DAPI exposure that fit within an established size-exclusion parameter. Using the mask as a template, cells with an overlapping signal in rhodamine for Ki67 positive nuclei are classified as positive or negative according to a threshold for signal intensity that is predetermined by eye. The advantages of this automated counting system are increased accuracy and decreased observer subjectivity. The potential limitation is that the signal intensity threshold is set and those nuclei that have positive but dim staining was not included. The error is systematic, and still small compared to other biases introduced with manual counting. To minimize this potential error, signal intensities are set using negative and positive controls for batches of slides stained at the same time using the same reagents. Thus, each batch is processed independently. TUNEL positive nuclei were manually verified to account for the variation in morphology of apoptotic cells including chromosomal condensation, blebbing, and cell shrinkage.

**Confocal Microscopy**

A Zeiss LSM 410 inverted laser scanning confocal microscope equipped with an external argon/krypton laser was used to acquire immunofluorescence images from thin sections of 3D lrECM cultures and breast cancer xenografts. A Zeiss Fluor x 40 (1.3 numerical aperture) objective was used, and images were captured at the colony mid-section for 3D lrECM cultures and breast cancer xenografts. The relative immunofluorescence intensity of images was

standardized by comparing only slides that were processed simultaneously under identical conditions.

**Statistical Analysis**

For Ki-67 and TUNEL counts in 3D lrECM, each culture condition, eg) each dose of AIIB2 or IgG and each dose of IR in both sequences) was compared in pair-wise fashion and Chi-square statistics were calculated for significant differences between groups. A p-value of $<0.05$ was considered to be an association that had a 95% probability of not being due to chance alone.

We estimated the numbers of animals needed for each experiment based on our prior experience with the MCF-7 xenograft models (19). The coefficient of variation for tumor volume using MCF-7 xenograft tumors is approximately 0.4. Assuming equal sample sizes and a two-sample student t-test, we estimated that 8 mice per group were needed in order to have 80% power (with a type 1 error of 5%) to detect a difference of 60% in mean volume between groups. In our first experiment, we started with 14 animals per group with planned animal sacrifice at different time points for biochemical analysis so that at 4 weeks, 8 animals per group would be remaining. Repeat verification experiments were performed with n=8 animals per group (data not shown). For tumor volume data, multivariate analysis of variance (MANOVA) was used for analysis at each time point. For each dose of AIIB2 or control IgG *in vivo*, a two-sided pair-wise student's t-test or chi-square comparison was used to analyze differences between TUNEL and Ki-67 expression. MINITAB (Minitab, Inc.) statistical software was used for all calculations.

## Results

### β1 integrin inhibition and IR are pro-apoptotic in malignant breast cell colonies and non-malignant cells in 2D, but not in acini-like structures in 3D lrECM

The original 3D assay developed by Petersen and Bissell laboratories (26) consisted of breast cells suspended in a laminin-rich extracellular matrix. Under these conditions, non-malignant and malignant cells can be rapidly and robustly distinguished from each other (26). We modified this assay to use as a screen for novel therapies and showed that it could be used as a surrogate to discriminate between normal and malignant tissue response to β1 integrin inhibitory antibody *in vivo* (Park et al 2006).

In the present study, we used the modified 3D lrECM assay to compare apoptotic response of malignant colonies and non-malignant acini to IR with and without β1 integrin inhibitory antibody. We treated the preformed S1 and T4-2 structures with 8 Gy IR or 0.08 mg/ml β1 integrin inhibitory antibody (AIIB2) alone or in combination where AIIB2 was added to the culture medium for 24 hours and the media was changed prior to IR exposure. The T4-2 cultures exhibited significant apoptosis compared to S-1 cultures after a single dose of 8 Gy, and the response was enhanced with the addition of AIIB2 (Figure 1B). In contrast, on standard 2D tissue culture plastic, FACS analysis for TUNEL or Annexin V showed that both non-malignant S-1 and malignant T4-2 cells had similar apoptotic responses to 8 Gy of IR regardless of the presence or absence of AIIB2 (Figure 1A). Furthermore, cellular reproductive capacity following IR

exposure (0-8 Gy) assessed by colony forming assays showed even more radiosensitivity in S1 compared to T4-2 cells (Supplemental Figure 1).

**β1 integrin inhibition administered after ionizing radiation optimally enhances apoptosis associated with a downregulation of Akt activity in 3D lrECM**

IR has been shown to upregulate β1 integrin expression in lung cancer cells in 2D (non malignant cells were not tested in this study) and breast cell lines in 3D lrECM (3, 5). Since we found previously that continuous AIIB2 treatment compared to 24 hour exposure was more effective in killing cancer cells, with little or no effect on S-1 colonies (19), we added AIIB2 to the medium each time the medium was changed until cultures were harvested. This protocol significantly increased apoptosis in T4-2 breast cancer cells in 3D lrECM post-IR, (Supplemental Figure 2A) without significantly affecting S-1 non-malignant acini (Supplemental Figure 2B).

To determine whether these findings were generalizable to other breast cancer cell lines, we used MCF-7 cells, a widely used model for breast cancer. In addition, to determining the optimal sequence of therapy, we treated 3D lrECM cultures with AIIB2 both before and after exposure to IR (Figure 2A). Compared to colonies that were treated with IR and a non-specific antibody control, colonies treated with combined IR and AIIB2 in either sequence showed an appreciable decrease in total cell numbers (data not shown) and a significant increase in apoptosis (assayed by TUNEL) compared to IR alone (Figure 2B). The observed

differences with untreated control were larger when IR was given before AIIB2; however, the data did not reach statistical significance to a level of 95% certainty in 2 of 4 experiments.

Using 2D cultures of small cell lung cancer and MDA-MB-231 breast cancer cell lines (did not include normal controls), others have shown that β1 integrin mediates resistance to apoptosis after cytotoxic insults, an effect mediated by a number of mechanisms including upregulation of Akt signaling (10, 13). Akt is a serine-threonine kinase that acts immediately downstream of phosphatidyl inositol-3 (PI3) kinase as a mediator of cell survival post IR (27-29). Akt activity was upregulated following IR in MCF-7 breast cancer cells in 3D lrECM measured by the increase in phosphorylation of serine 473 on Akt (p-S473 Akt) using western blots. Upregulation post-IR was dose-dependent (Figure 2C) indicating that IR induced an increase in Akt activity that could potentially be targeted by β1 integrin inhibitory antibodies. To address this possibility further, we assayed 3D lrECM cultures for levels of p-S473 Akt after exposure either to IR and control IgG antibodies or a combination of IR and AIIB2 with the latter applied both before and after IR. We found that down regulation of Akt activity occurred when AIIB2 was administered post-IR, Figure 2C. Interestingly, Akt activity after 6 hours of AIIB2 treatment alone did not decline once the cancer cells had already formed colonies (Figure 2C). We further verified these results in T4-2 cells in 3D lrECM (Supplemental Figure 2C) and found no significant change in Akt activity after similar treatment of non-malignant S-1 structures (Supplemental Figure 2D).

**IR-induced Akt effects could be overcome by application of β1 integrin inhibitory antibody**

In order to evaluate whether apoptosis induced by β1 integrin inhibition or IR operated directly through Akt signaling, we utilized T4-2 cells transfected with a constitutively activated, myristoylated form of Akt (myr-Akt) (30, 31), (the construct was a kind gift of R. Roth,(32)) Figure 3A. We measured apoptosis using TUNEL in T4-2 myrAkt colonies after either IR alone or in combination with 0.08 mg/ml AIIB2 -the dose used previously to induce apoptosis in several breast cancer cell lines in 3D lrECM (19). In contrast to T4-2 vector controls, which showed increased apoptosis after IR plus 0.08 mg/ml AIIB2, T4-2 myrAkt colonies were refractory to this treatment (Figure 3B).

We reasoned that if Akt activity was responsive to β1 integrin signaling, then increasing β1 integrin inhibition could abrogate Akt signaling even in myr-AKt cells. A 3-fold increase in AIIB2 (0.24 mg/ml) elicited apoptosis in T4-2 myr-Akt cells in an IR-dose dependent manner in 3D lrECM (Figure 3C). To determine if this apoptotic response correlated with downregulation of Akt signaling, we measured p-S473 Akt and phosphorylated threonine 1462 TSC-2 (p-Thr1462 TSC-2), a downstream target of Akt activity (32). Concordant with the results observed in MCF-7 cells, Akt was upregulated 6 hours after IR alone in T4 myr-Akt, (Figure 3D). Moreover, treatment with these higher doses of AIIB2 corresponded to downregulation in p-S473 Akt and p-Thr1462 TSC-2. Taken together, these data strongly suggest that IR resistance is in part

mediated by activation of β1 integrin and a subsequent increase in Akt signaling both of which could be abrogated by β1 integrin inhibition.

**Combining β1 integrin inhibition with IR treatment *in vivo* allows reduction of the effective dose of IR**

Given the promising results in 3D lrECM, we asked whether these data could be validated *in vivo*. Following implantation of MCF-7 cells into the rear flank of female athymic nu-/- mice (n=14 per group), animals were subsequently randomized to receive either IR and control IgG, IR followed by AIIB2 or AIIB2 followed by IR, as described in Material and Methods (Figure 4A). Overall, the addition of AIIB2 to IR enhanced tumor growth inhibition compared to either treatment alone (Supplemental Figure 3). Remarkably, we found that animals that received 2 Gy followed by AIIB2, had similar tumor growth inhibition to those that received 8 Gy with control antibody ($p<0.014$; Figure 4B). We measured apoptosis at 24 hours after the final treatment in each group and found that tumors treated with 2 Gy plus AIIB2 also had a higher rate of apoptosis compared to other groups (Figure 4B).

To verify whether Akt activity was downregulated by combined treatment as we had observed in 3D lrECM, we assayed whole tumor cell lysates for evidence of Akt activity by probing for phosphorylation of S473 Akt. Again, the *in vivo* results replicated the findings in 3D: we observed an increase in AKT activity associated with IR dose, which was down modulated by the addition of AIIB2 after IR (Figure 4C).

## Discussion

Here we report promising results combining β1 integrin inhibitory antibody with IR to decrease the total effective radiation dose and to maximize the efficacy of treatment by sensitizing the tumor, but not normal organs, to IR. Our increasing awareness of the global effects of IR on tissues, and the role of the microenvironment on modifying cellular response to IR (2, 33) are pointing to the necessity of reducing IR effective doses if at all possible by advancing our knowledge and providing novel therapeutic targets. β1 integrin plays a multifaceted role in cancer progression and resistance to cytotoxic treatment including IR. We have shown previously that β1 integrin inhibitory antibody, AIIB2, can revert the malignant phenotype of cells in 3D lrECM (21) and enhance breast cancer cell death in xenografts while sparing nonmalignant acini in culture and normal organs *in vivo* (19). Here we show that AIIB2 post-IR, selectively enhances apoptosis in breast cancer cells but not non-malignant acini in 3D lrECM organotypic cultures, and that antibody combined with low doses of IR can achieve similar inhibition in tumor growth to single, but much larger doses of IR *in vivo*. In addition, we find that enhanced apoptosis after combined treatment is associated with down modulation in Akt signaling, again both in 3D cultures and *in vivo*. Importantly, when we assayed for apoptosis and reproductive death in standard 2D tissue culture, we were unable to discriminate between malignant and non-malignant cells. These data corroborate our previously published data on treatment with single chemical agents (19, 34) and indicate that the intrinsic radiosensitivity of both normal and cancer cells are modified also in the context of

the 3D structures. Importantly we verify here that the 3D lrECM assay is a useful and faithful surrogate for predicting differences in normal and malignant tissue response *in vivo*.

We had shown previously that IR induces heritable and global changes in cell-ECM interactions, and specifically in β1 integrin expression, in human mammary epithelial cells cultured in 3D lrECM. We also have observed activation of β1 integrins in breast cancer cells post-IR (unpublished) corroborating reports by others of integrin activation in irradiated tumors (4, 5, 35). We reasoned that if β1 integrin were upregulated by IR, then AIIB2 would be more effective post-IR than pre-IR because of increased epitope accessibility to antibody binding. To test whether there was an optimal sequencing of treatment, we used the 3D lrECM assay where cancer cells were cultured to form tumor-like colonies and then treated with either AIIB2, 24 hours prior to IR or 24 hours post-IR. Both sequences resulted in significantly greater cell death ($p<0.05$) compared to IR alone without significant toxicity to non-malignant cells. Although there was a trend that favored sequencing IR followed by AIIB2, this did not achieve a statistical significance between the two treatment regimes over multiple repeated experiments. One of the likely reasons for this finding is that the magnitude of effect of AIIB2 alone was greater than a measurable difference attributed solely to the sequence of treatment. Importantly, AIIB2 was maintained continuously in the 3D lrECM cultures as it would be also *in vivo*. Studies that examined the effect of sequencing PI3 kinase inhibitor, LY294002, in breast cancer cells in 2D culture (36) reported an optimal increase in apoptosis

after combined IR and LY when LY was given both pre- and post-IR. However the effects of the inhibitor and IR in non-malignant cells was not reported. Another group (37) showed that LY294002 given pre-IR in HeLa cells was significantly better than post-IR. These results are not directly comparable to ours since the culture models and mechanism of action of Akt pathway inhibition are different in 2D and 3D; however, they do indicate that sequencing may play an important role in optimally delivering combined treatments based on the mechanisms of interaction of the inhibitor and IR and the context in which IR and the drug are delivered.

PI3 kinase inhibitors have long been known to sensitize to, or work in combination with, IR to enhance apoptosis in several cancer cell types in cultured cell lines. Akt is emerging as a central mediator of resistance both from studies showing the radiosensitizing effect of PI3 kinase inhibition (5, 38) and as a major effector of PI3 kinase, the activity of which is modified by multiple cell surface receptors including growth factors and integrins. In our 3D lrECM model, AIIB2 post-IR resulted in down regulation of Akt signaling, which was associated with enhanced apoptosis.

Our data complement those of others who showed that survival of bladder cancer cells harboring a mutation in *ras* was significantly decreased after combined treatment with LY294002 and IR, although these investigators reported no significant benefit of LY alone either in 2D cultures or *in vivo* (16, 39). Others also have reported a synergistic effect of LY294002 and IR for glioblastoma multiforme xenografts (27). Although dose-limiting toxicity and pharmacokinetics

limit LY294002 as a viable drug in humans, these studies highlight the importance of targeting Akt in conjunction with IR. In addition, Akt has been shown to be a promising target in cancer cells downstream of integrins and growth factor pathways post IR (17). Thus, multiple pathways at the cell surface converge at Akt via PI3 kinase, a central mediator of cancer cell survival, which may be targeted simultaneously to enhance therapeutic efficacy. Our data point to the existence of an IR-dependent survival pathway mediated by Akt that is down modulated with β1 integrin inhibition. It is quite possible that IR affects polarity pathways involving Rac 1 (32), which was shown also to affect radiation–induced apoptosis (40, 41).

We found that the addition of AIIB2 treatment to IR *in vivo* resulted in significant improvement in inhibition of tumor growth by allowing a much smaller dose of IR (2 Gy) but reaching the same end point of higher doses of IR alone (8 Gy). To our knowledge, this is the first report of a β1 integrin inhibitor used in conjunction with IR in a therapeutic context *in vivo*. There was a modest improvement in tumor growth inhibition associated with the addition of AIIB2 to 8 Gy compared to 8 Gy alone. But improvement on 2GY of radiation was considerable. These data suggest that there may be an IR dose threshold above which the addition of AIIB2 has decreasing value in enhancing tumor cell death. We acknowledge that the doses and single fractions used in these experiments may not be the optimal dosing and sequencing in humans, however these data provide proof of principle that the combination of β1 integrin inhibition and IR are a promising novel strategy for breast cancer radiotherapy.

Several questions remain unanswered, and are currently undergoing active investigation by us and others. Clinically, fractionated IR is used to minimize normal tissue damage. It is unclear how β1 integrin inhibitory agents may be optimized with fractionated therapy, and to what degree the total necessary IR dose may be modified to achieve maximal tumor control. A role for β1 integrin- and Akt-mediated resistance post-IR is an active area of investigation. Our data indicate that there are alternate pathways that act in the presence of IR that could promote survival via Akt. Together, our findings show great promise for the combination of β1 integrin inhibitory agents and IR, and provide a rationale for combining multiple agents that target the Akt/PI3 kinase pathways post IR.

**Acknowledgements**

We thank Stephanie Kim and Richard Y. Lee for technical assistance. Support for this research was provided by the UCSF CIRP (CP) NIH P50 SPORE CA CA58207-08 (CP); the U.S. Department of Energy, Office of Biological and Environmental Research (DE-AC02-05CH11231 to MJB); NIH/NCI (CA64786-09 to MJB); an Innovator Award from the U.S. Department of Defense Breast Cancer Research Program (DAMD17-02-1-0438 to MJB).

## References


1. Park CC, Mitsumori M, Nixon A, Recht A, Connolly J, Gelman R, et al. Outcome at 8 years after breast-conserving surgery and radiation therapy for invasive breast cancer: influence of margin status and systemic therapy on local recurrence. J Clin Oncol 2000;18(8):1668-75.
2. Barcellos-Hoff MH, Park C, Wright EG. Radiation and the microenvironment - tumorigenesis and therapy. Nat Rev Cancer 2005;5(11):867-75.
3. Park CC, Henshall-Powell RL, Erickson AC, Talhouk R, Parvin B, Bissell MJ, et al. Ionizing radiation induces heritable disruption of epithelial cell interactions. Proc Natl Acad Sci U S A 2003;100(19):10728-33.
4. Onoda JM, Piechocki MP, Honn KV. Radiation-induced increase in expression of the alpha IIb beta 3 integrin in melanoma cells: effects on metastatic potential. Radiat Res 1992;130(3):281-8.
5. Cordes N, Blaese MA, Meineke V, Van Beuningen D. Ionizing radiation induces up-regulation of functional beta1-integrin in human lung tumour cell lines in vitro. Int J Radiat Biol 2002;78(5):347-57.
6. Damiano JS, Hazlehurst LA, Dalton WS. Cell adhesion-mediated drug resistance (CAM-DR) protects the K562 chronic myelogenous leukemia cell line from apoptosis induced by BCR/ABL inhibition, cytotoxic drugs, and gamma-irradiation. Leukemia 2001;15(8):1232-9.
7. Damiano JS, Cress AE, Hazlehurst LA, Shtil AA, Dalton WS. Cell adhesion mediated drug resistance (CAM-DR): role of integrins and resistance to apoptosis in human myeloma cell lines. Blood 1999;93(5):1658-67.
8. Cordes N, Seidler J, Durzok R, Geinitz H, Brakebusch C. beta1-integrin-mediated signaling essentially contributes to cell survival after radiation-induced genotoxic injury. Oncogene 2006;25(9):1378-90.
9. Cordes N, Meineke V. Cell adhesion-mediated radioresistance (CAM-RR). Extracellular matrix-dependent improvement of cell survival in human tumor and normal cells in vitro. Strahlenther Onkol 2003;179(5):337-44.
10. Hodkinson PS, Elliott T, Wong WS, Rintoul RC, Mackinnon AC, Haslett C, et al. ECM overrides DNA damage-induced cell cycle arrest and apoptosis in small-cell lung cancer cells through beta1 integrin-dependent activation of PI3-kinase. Cell Death Differ 2006;13(10):1776-88.
11. Hynes RO. Integrins: bidirectional, allosteric signaling machines. Cell 2002;110(6):673-87.
12. Giancotti FG, Ruoslahti E. Integrin signaling. Science 1999;285(5430):1028-32.
13. Aoudjit F, Vuori K. Integrin signaling inhibits paclitaxel-induced apoptosis in breast cancer cells. Oncogene 2001;20(36):4995-5004.
14. Morozevich GE, Kozlova NI, Preobrazhenskaya ME, Ushakova NA, Eltsov IA, Shtil AA, et al. The role of beta1 integrin subfamily in anchorage-dependent apoptosis of breast carcinoma cells differing in multidrug resistance. Biochemistry (Mosc) 2006;71(5):489-95.

15. Yao ES, Zhang H, Chen YY, Lee B, Chew K, Moore D, et al. Increased beta1 integrin is associated with decreased survival in invasive breast cancer. Cancer Res 2007;67(2):659-64.
16. Gupta AK, Cerniglia GJ, Mick R, Ahmed MS, Bakanauskas VJ, Muschel RJ, et al. Radiation sensitization of human cancer cells in vivo by inhibiting the activity of PI3K using LY294002. Int J Radiat Oncol Biol Phys 2003;56(3):846-53.
17. Hallahan D, Geng L, Qu S, Scarfone C, Giorgio T, Donnelly E, et al. Integrin-mediated targeting of drug delivery to irradiated tumor blood vessels. Cancer Cell 2003;3(1):63-74.
18. Seidler J, Durzok R, Brakebusch C, Cordes N. Interactions of the integrin subunit beta1A with protein kinase B/Akt, p130Cas and paxillin contribute to regulation of radiation survival. Radiother Oncol 2005;76(2):129-34.
19. Park CC, Zhang H, Pallavicini M, Gray JW, Baehner F, Park CJ, et al. Beta1 integrin inhibitory antibody induces apoptosis of breast cancer cells, inhibits growth, and distinguishes malignant from normal phenotype in three dimensional cultures and in vivo. Cancer Res 2006;66(3):1526-35.
20. Briand P, Petersen OW, Van Deurs B. A new diploid nontumorigenic human breast epithelial cell line isolated and propagated in chemically defined medium. In Vitro Cell Dev Biol 1987;23(3):181-8.
21. Weaver VM, Petersen OW, Wang F, Larabell CA, Briand P, Damsky C, et al. Reversion of the malignant phenotype of human breast cells in three-dimensional culture and in vivo by integrin blocking antibodies. J Cell Biol 1997;137(1):231-45.
22. Hall DE, Reichardt LF, Crowley E, Holley B, Moezzi H, Sonnenberg A, et al. The alpha 1/beta 1 and alpha 6/beta 1 integrin heterodimers mediate cell attachment to distinct sites on laminin. J Cell Biol 1990;110(6):2175-84.
23. Tomaselli KJ, Damsky CH, Reichardt LF. Purification and characterization of mammalian integrins expressed by a rat neuronal cell line (PC12): evidence that they function as alpha/beta heterodimeric receptors for laminin and type IV collagen. J Cell Biol 1988;107(3):1241-52.
24. Werb Z, Tremble PM, Behrendtsen O, Crowley E, Damsky CH. Signal transduction through the fibronectin receptor induces collagenase and stromelysin gene expression. J Cell Biol 1989;109(2):877-89.
25. Wang F, Weaver VM, Petersen OW, Larabell CA, Dedhar S, Briand P, et al. Reciprocal interactions between beta1-integrin and epidermal growth factor receptor in three-dimensional basement membrane breast cultures: a different perspective in epithelial biology. Proc Natl Acad Sci U S A 1998;95(25):14821-6.
26. Schafer JM, Bentrem DJ, Takei H, Gajdos C, Badve S, Jordan VC. A mechanism of drug resistance to tamoxifen in breast cancer. J Steroid Biochem Mol Biol 2002;83(1-5):75-83.
27. Edwards E, Geng L, Tan J, Onishko H, Donnelly E, Hallahan DE. Phosphatidylinositol 3-kinase/Akt signaling in the response of vascular endothelium to ionizing radiation. Cancer Res 2002;62(16):4671-7.
28. Nakamura JL, Karlsson A, Arvold ND, Gottschalk AR, Pieper RO, Stokoe D, et al. PKB/Akt mediates radiosensitization by the signaling inhibitor LY294002 in human malignant gliomas. J Neurooncol 2005;71(3):215-22.

29. Zingg D, Riesterer O, Fabbro D, Glanzmann C, Bodis S, Pruschy M. Differential activation of the phosphatidylinositol 3'-kinase/Akt survival pathway by ionizing radiation in tumor and primary endothelial cells. Cancer Res 2004;64(15):5398-406.
30. Kohn AD, Barthel A, Kovacina KS, Boge A, Wallach B, Summers SA, et al. Construction and characterization of a conditionally active version of the serine/threonine kinase Akt. J Biol Chem 1998;273(19):11937-43.
31. Liu H, Radisky DC, Wang F, Bissell MJ. Polarity and proliferation are controlled by distinct signaling pathways downstream of PI3-kinase in breast epithelial tumor cells. J Cell Biol 2004;164(4):603-12.
32. Hay N. The Akt-mTOR tango and its relevance to cancer. Cancer Cell 2005;8(3):179-83.
33. Barcellos-Hoff MH. It takes a tissue to make a tumor: epigenetics, cancer and the microenvironment. J Mammary Gland Biol Neoplasia 2001;6(2):213-21.
34. Weaver VM, Lelievre S, Lakins JN, Chrenek MA, Jones JC, Giancotti F, et al. beta4 integrin-dependent formation of polarized three-dimensional architecture confers resistance to apoptosis in normal and malignant mammary epithelium. Cancer Cell 2002;2(3):205-16.
35. Handschel J, Prott FJ, Sunderkotter C, Metze D, Meyer U, Joos U. Irradiation induces increase of adhesion molecules and accumulation of beta2-integrin-expressing cells in humans. Int J Radiat Oncol Biol Phys 1999;45(2):475-81.
36. Liang K, Jin W, Knuefermann C, Schmidt M, Mills GB, Ang KK, et al. Targeting the phosphatidylinositol 3-kinase/Akt pathway for enhancing breast cancer cells to radiotherapy. Mol Cancer Ther 2003;2(4):353-60.
37. Lee CM, Fuhrman CB, Planelles V, Peltier MR, Gaffney DK, Soisson AP, et al. Phosphatidylinositol 3-kinase inhibition by LY294002 radiosensitizes human cervical cancer cell lines. Clin Cancer Res 2006;12(1):250-6.
38. Brognard J, Clark AS, Ni Y, Dennis PA. Akt/protein kinase B is constitutively active in non-small cell lung cancer cells and promotes cellular survival and resistance to chemotherapy and radiation. Cancer Res 2001;61(10):3986-97.
39. Kim IA, Bae SS, Fernandes A, Wu J, Muschel RJ, McKenna WG, et al. Selective inhibition of Ras, phosphoinositide 3 kinase, and Akt isoforms increases the radiosensitivity of human carcinoma cell lines. Cancer Res 2005;65(17):7902-10.
40. Choi JA, Park MT, Kang CM, Um HD, Bae S, Lee KH, et al. Opposite effects of Ha-Ras and Ki-Ras on radiation-induced apoptosis via differential activation of PI3K/Akt and Rac/p38 mitogen-activated protein kinase signaling pathways. Oncogene 2004;23(1):9-20.
41. Choi SY, Kim MJ, Kang CM, Bae S, Cho CK, Soh JW, et al. Activation of Bak and Bax through c-abl-protein kinase Cdelta-p38 MAPK signaling in response to ionizing radiation in human non-small cell lung cancer cells. J Biol Chem 2006;281(11):7049-59.

**Figure 1. AIIB2 selectively enhances IR-induced apoptosis in malignant but not non-malignant breast cells assayed in 3D lrECM culture.**

(A1) Experimental schema in 2D culture: S-1 and T4-2 cells were treated with AIIB2 and IR on Day 2 and 3 after plating and assayed for apoptosis on Day 4. (A2) Phase contrast micrographs of S-1 and T4-2 cultures after treatment with IR alone (top panel) or in combination with AIIB2 (bottom panel). (A3) Apoptosis measured by TUNEL and Annexin V show increased apoptosis with the addition of AIIB2 and IR, bars=mean +SE, *p<0.05, Chi square. (B1) Experimental schema in 3D lrECM culture: non-malignant S-1 acini were treated with antibody and IR on Day 6-7 and malignant colonies were treated with antibody and IR on Day 4-5; all cultures were assayed at 72 hours post-treatment. (B2) Phase contrast micrographs of 3D lrECM cultures after treatment with IR (top panel) or in combination with AIIB2 (bottom panel), bar=20um. Confocal images of TUNEL positive cells are shown in the inset in green, DAPI nuclei are shown in blue, bar=10um. (B3) Percentage of TUNEL positive cells shows that apoptosis was enhanced by combined therapy in malignant T4-2 cells but not non-malignant S-1 acini, bars=mean +SE, *p<0.05, Chi square.

**Figure 2**. **β1 integrin inhibition optimally enhances apoptosis post-IR in 3D lrECM in an Akt dependent manner.**

(A) Experimental schema: MCF-7 cells were allowed to form malignant colonies in 3D lrECM for 3 days and then were treated with IR+/- AIIB2 as shown. (B) Apoptosis was measured by counting TUNEL-positive nuclei, bars=mean + SE,

*= p<0.05, Chi-square. Results are reflective of n=3 experiments. (C) Total levels of AKT and pS473 Akt were detected by Western blotting of total cell lysates. Quantitation is relative to β-actin.

**Figure 3**. **Akt-mediated resistance to apoptosis post-IR is abrogated by AIIB2 in a dose-dependent manner**

(A) Western blot shows the presence of constitutively active Akt in transfected T4-2 cells versus vector controls. (B) T4 myr-AKT cells are resistant to apoptosis after IR and 0.08 mg/ml AIIB2, bars =mean + SD. (C) Apoptosis is significantly increased with doses of 0.24 mg/ml AIIB2 and greater (> 3X's the doses necessary to induce apoptosis in vector control cells), bars =mean + SD, *=p<0.05, Chi-square. (D) Western blot (and quantification) of phospho-Akt, and phospho-Thr 1462 TSC2 are increased with IR or AIIB2 alone, but decreased when treated with a combination of 0.24 mg/ml of AIIB2 and IR.

**Figure 4. 2 Gy IR followed by AIIB2 is more effective than AIIB2 or 2 Gy alone**

(A) Experimental schema: MCF-7 xenograft bearing mice (n=14) were randomized to receive either IR plus control antibody, IR plus AIIB2 or AIIB2 + IR. (B) Comparison of tumor growth curves shows that 2Gy IR→AIIB2 resulted in greater time to tumor progression (400 $mm^3$ than 2 Gy alone, *=log rank p<0.014, and was similar in efficacy to 8 Gy alone. (B1) Comparison of apoptosis

measured by TUNEL assay at 24 hours after the addition of IR or AIIB2, bars = mean + SEM.(C) Western blot shows that 3+

+9IR plus AIIB2 is associated with down regulation of p-S473Akt activity *in vivo.*

**Supplemental Figure 1. Non-malignant S-1 cells are more radiosensitive than T4-2 malignant cells in 2D colony formation assays**

Colony formation was determined after single doses of IR from 0-8 Gy with or without AIIB2. S-1 cells were more radiosensitive than T4-2 cells after IR, and the addition of AIIB2 showed a trend for decrease reproductive capacity in T4-2 cells post-IR.

**Supplemental Figure 2**. **β1 integrin inhibition enhances apoptosis post-IR in an Akt dependent manner in T4-2 breast cancer cells but not S-1 structures in 3D lrECM**(A) T4-2 control colonies were treated with IR (0, 2 or 8 Gy) with or without AIIB2 in 3D lrECM. The percentage of apoptotic cells significantly increased with the addition of AIIB2 post-IR. (B) Western blot for phosphorylated S473 Akt 6 hours after treatment showed an IR-dose dependent increase in Akt activity that is decreased with AIIB2 treatment. (C) S-1 non-malignant structures were treated with IR (0,2 or 8 Gy) with or without AIIB2 in 3D lrECM. The percentage of apoptotic cells was not significantly changed despite IR alone, AIIB2 alone or a combination of IR plus AIIB2. (D) Western blot shows no upregulation in p-AKT after IR or down regulation after addition of AIIB2.

**Supplemental Figure 3**. **Tumor growth inhibition by IR is enhanced by the addition of β1 integrin inhibitory antibody, AIIB2, in vivo**

(A) Experimental Schema. (B) IR alone resulted in significant inhibition of tumor growth after 2 and 8 Gy compared to Sham treated animals, *=p<0.05, Chi-square, bar=mean ± SE. (C) Treatment with 2 Gy IR→AIIB2 resulted in significant growth inhibition compared to Sham→AIIB2 treated animals, *=p<0.05, Chi-square, bar=mean ± SE. (D) Treatment with AIIB2→8 Gy showed a significant effect vs. control IgG, *=p<0.05, Chi-square, bar=mean ± SE. (E) Dual immunofluorescence for Ki-67 (red) and TUNEL (green) with DAPI nuclei (blue) in sections from MCF-7 xenograft tumors. (F) TUNEL analysis at 24 hours after treatment shows increased apoptosis after 2Gy→AIIB2, which was significantly greater than AIIB2→2Gy or 8 Gy +/- AIIB2, bar=mean + S.E., p<0.05, Chi-square. (gG) Ki-67 analysis at 24 hours after treatment showed decreasing proliferation with IR dose for treatment group IR→AIIB2, and the opposite trend for group receiving AIIB2→IR.

**Figure 1**. Inhibition of β1 integrin selectively enhances IR-induced apoptosis in malignant but not non-malignant breast cells assayed in 3D lrECM

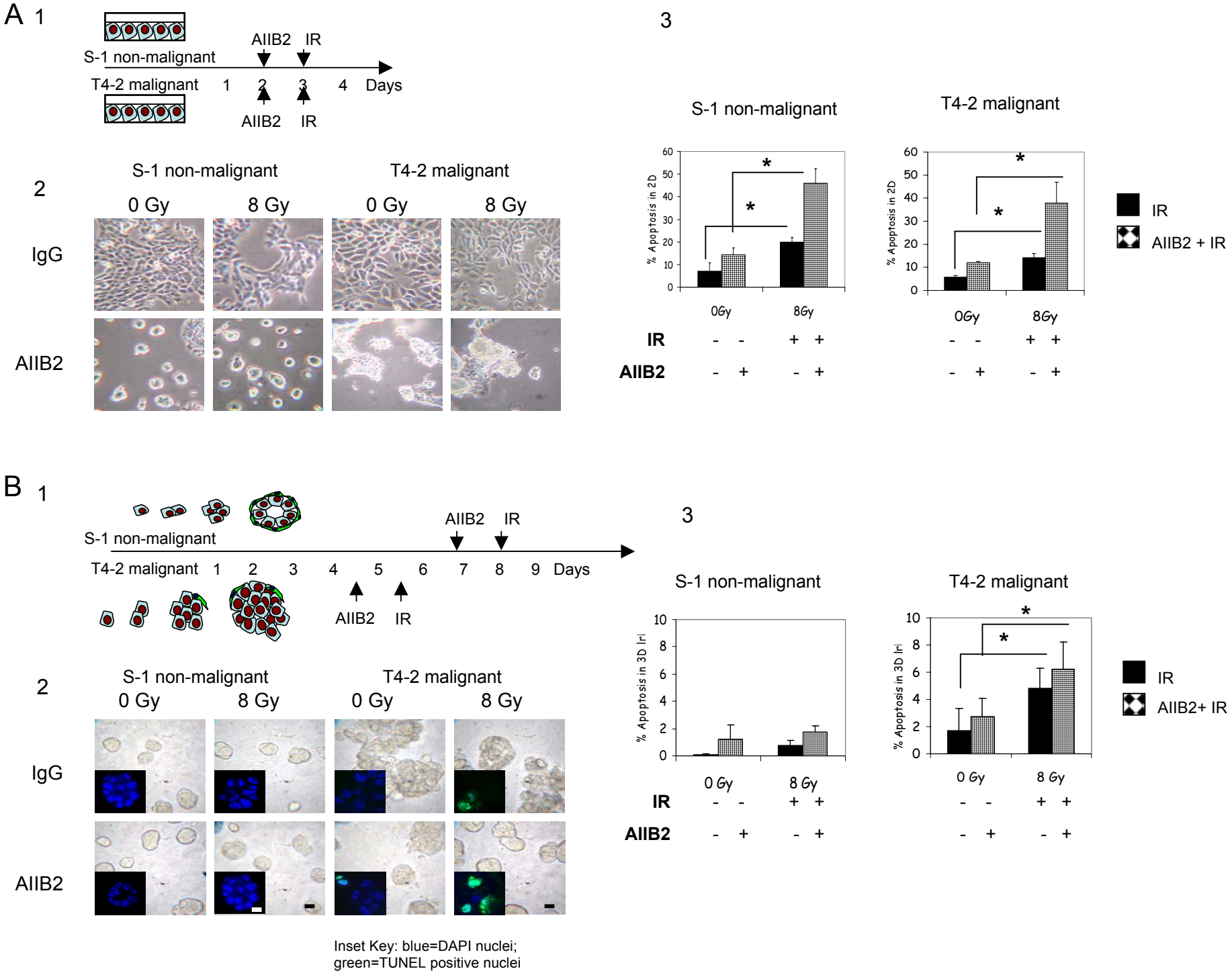


Inset Key: blue=DAPI nuclei;
green=TUNEL positive nuclei

**Figure 2**. β1 integrin inhibition optimally enhances apoptosis post-IR in 3D lrECM in an Akt-dependent manner

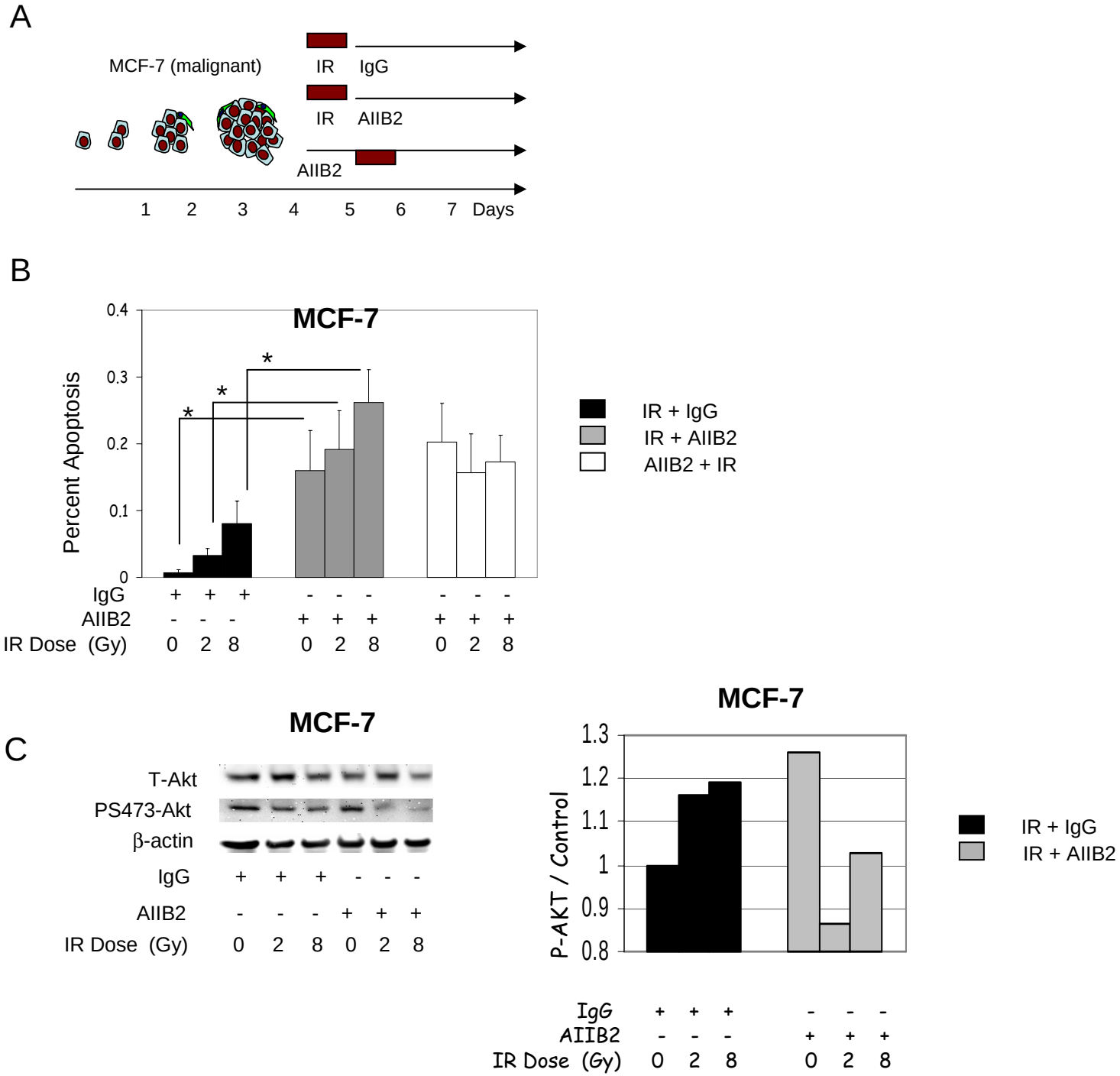

**Figure 3**. Akt-mediated resistance to apoptosis post-IR is abrogated by AIIB2 in a dose-dependent manner

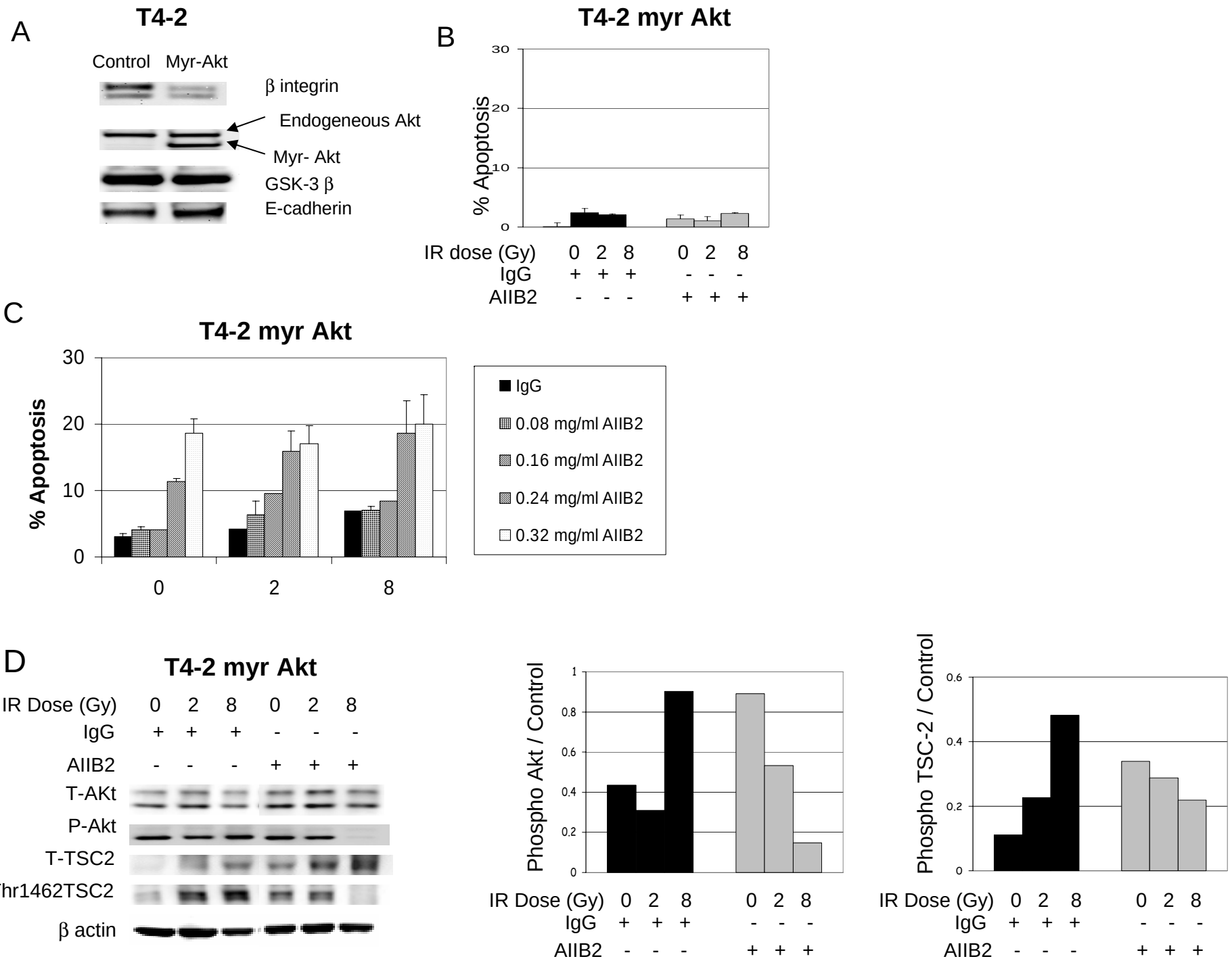

**Figure 4.** Combining β1 integrin inhibition with IR treatment *in vivo* allows for reduction of effective IR dose

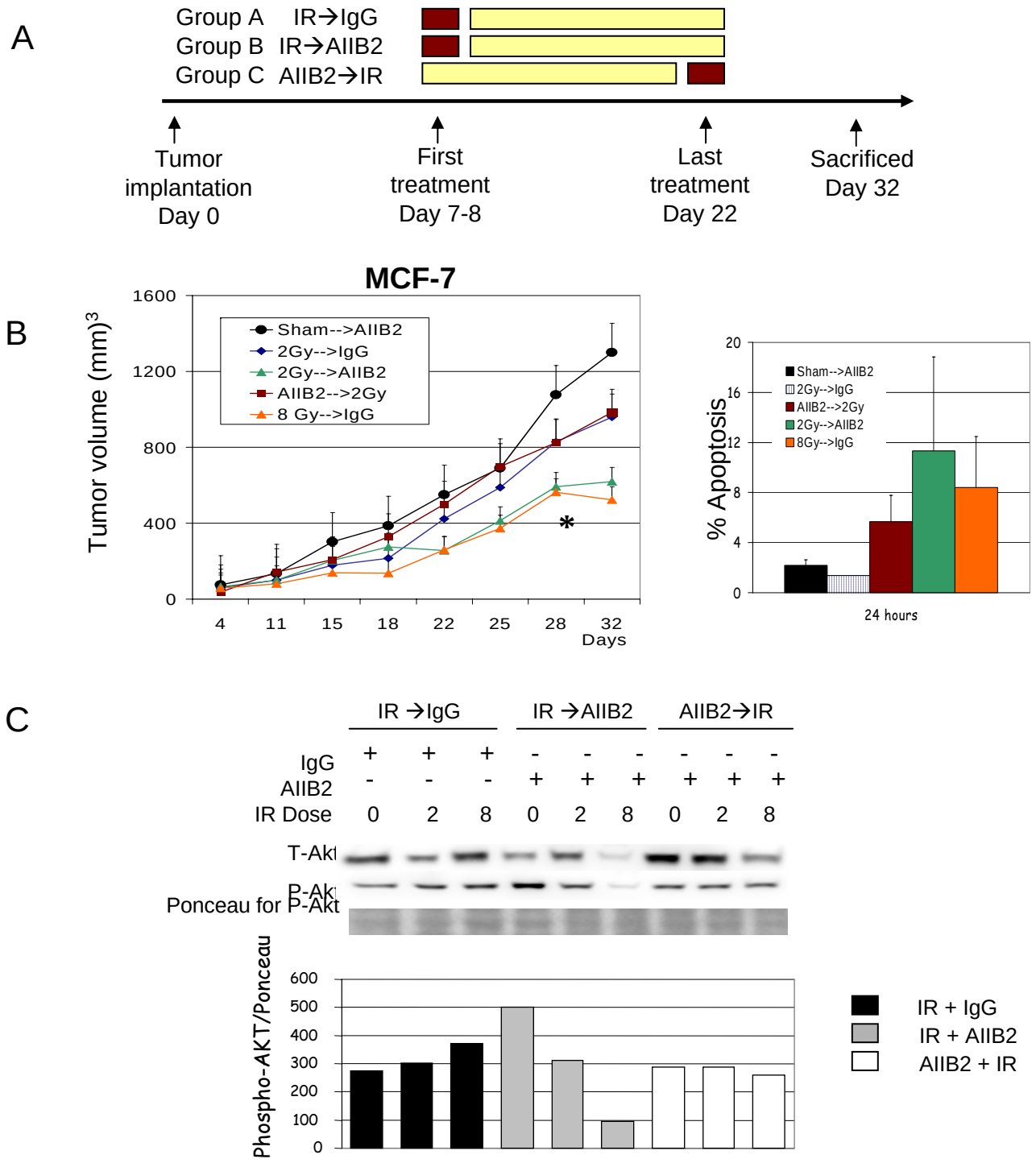

**Supplemental Figure 1**. Non-malignant S-1 breast epithelial cells are more radiosensitive than counterpart T4-2 malignant cells on colony forming assay in 2D culture

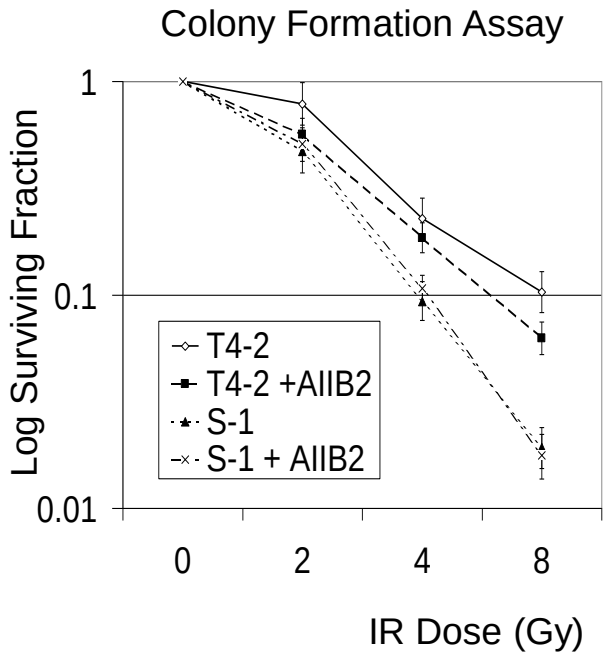

**Supplemental Figure 2**. β1 integrin inhibition enhances apoptosis post-IR in an Akt dependent manner in T4-2 breast cancer cells but not S-1 structures in 3D lrECM

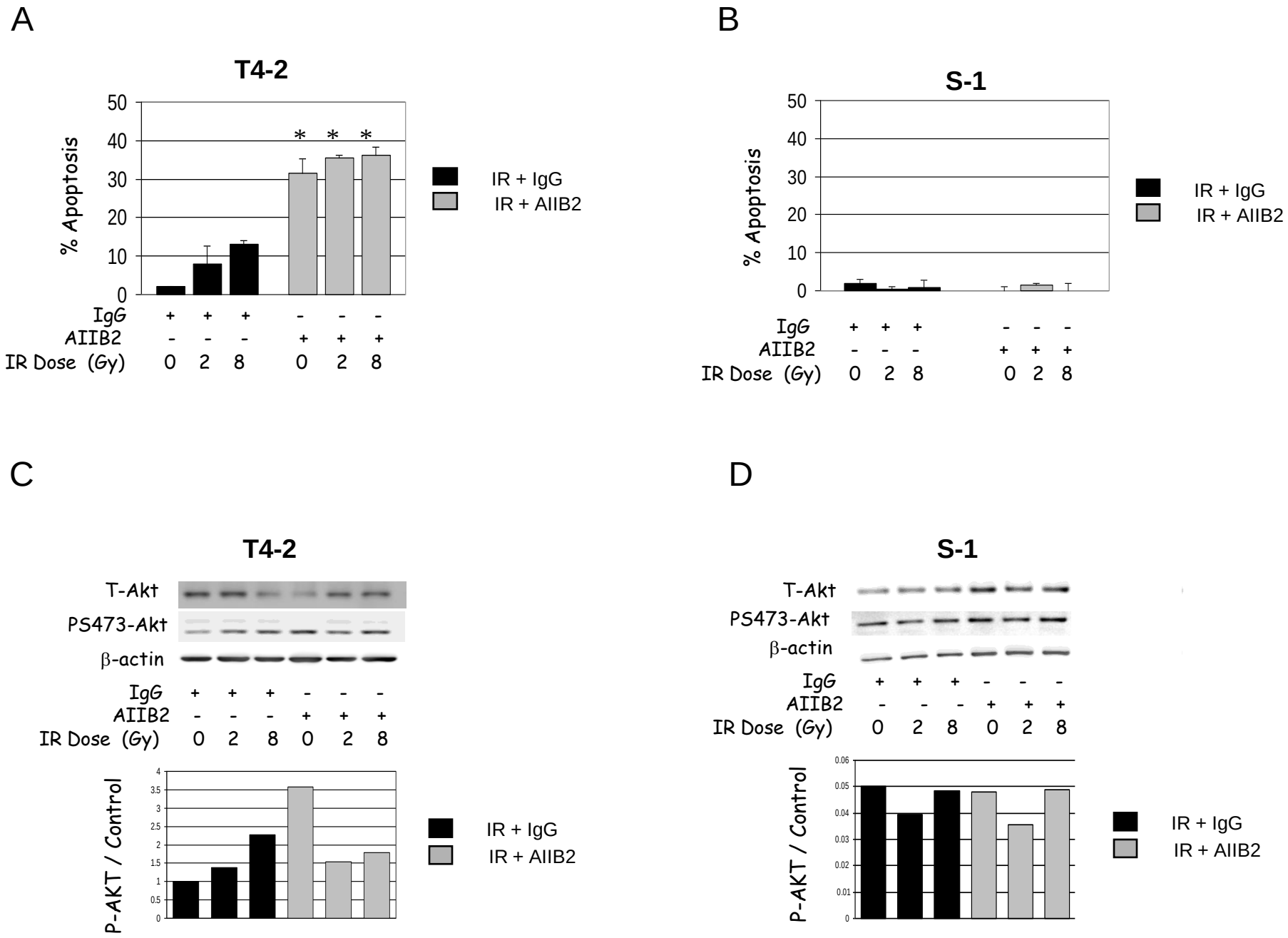

**Supplemental Figure 3**. Tumor growth inhibition by IR is enhanced by the addition of β1 integrin inhibitory antibody, AIIB2, *in vivo*